Current Titles

National Center for Electron Microscopy

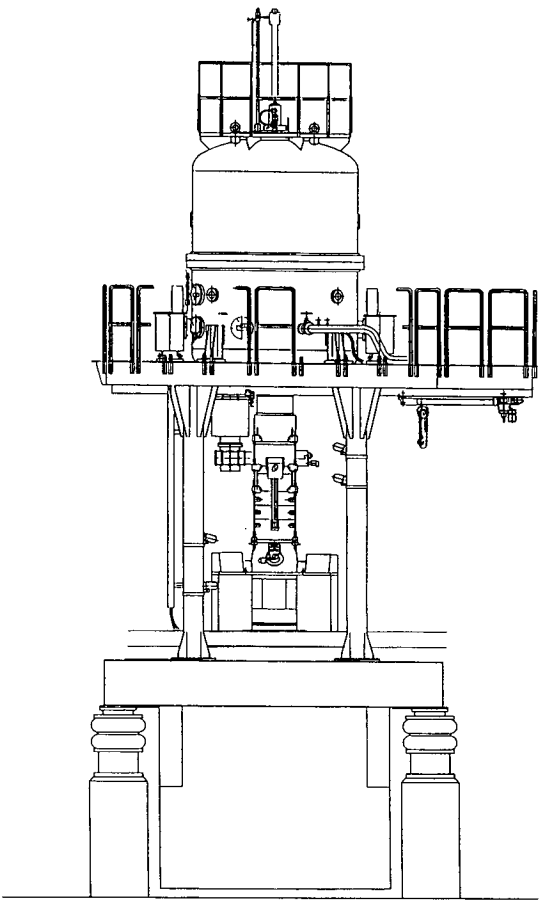

April 1993

PUB-719

DISCLAIMER

National Center for Electron Microscopy
U.C. Lawrence Berkeley Laboratory
1 Cyclotron Rd. Building 72
Berkeley CA 94720

National Center for Electron Microscopy
U.C. Lawrence Berkeley Laboratory
1 Cyclotron Rd. Building 72
Berkeley CA 94720

Please send a reprint of the paper(s):

Number	Author(s)	Title

Name_____ Date_____

Affiliation_____

Address_____

_____

Please send a reprint of the paper(s):

Number	Author(s)	Title

Name_____ Date_____

Affiliation_____

Address_____

_____

Current Titles

National Center for Electron Microscopy
Lawrence Berkeley Laboratory
University of California
Berkeley, California 94720

April 1993

PUB-719

The NCEM is supported by the Director, Office of Energy Research, Office of Basic Energy Sciences, Materials Sciences Division of the U.S. Department of Energy under Contract No. DE-AC03-76SF00098

This booklet is published for those interested in current research being conducted at the National Center for Electron Microscopy. The NCEM is a DOE-designated national user facility and is available at no charge to qualified researchers†. Access is controlled by a steering committee.
Interested researchers may contact Gretchen Hermes at (510) 486-5006 or address below for a User's Guide.

Copies of available papers in print can be ordered by copying and using the form at the end of this booklet or by using your own request card and sending to:

Theda Crawford
National Center for Electron Microscopy
Lawrence Berkeley Laboratory
One Cyclotron Rd., MS72
Berkeley, California, USA 94720

Articles are listed alphabetically by journal.

Legend:

Number = publication number

M = Manuscript, A = Abstract

R = Reprints, P = Preprints, No = None available

33427 M No
C.P. Burmester, L.T. Wille, and R. Gronsky

Computer Simulations of Growth Mechanisms in Y-Ba-Cu-O Thin Films

5th Int'l. Symp. on Superconductivity

The growth of epitaxial thin films of $YBa_2Cu_3O_7$ is studied by means of computer simulation of the deposition and diffusion of Y, Ba, and Cu oxide particles. The evolution process is modeled by means of a three-step Monte Carlo technique incorporating one sorption deposition mode and two modes of film annealing addressing surface and bulk diffusion. A systematic study of the effects of deposition rate and substrate temperature during in-situ film fabrication reveals that the kinetics of film growth can readily dominate the structural formation of the thin film leading to dramatic morphological transitions as a function of deposition conditions alone.

33821 A No
S. Paciornik, R. Kilaas, U. Dahmen and M.A. O'Keefe

A Method for Direct Measurements of Specimen Noise in HREM Images

Abstract for EMSA

High resolution electron microscopy (HREM) is a primary tool for studying the atomic structure of defects in crystals. However, the quantitative analysis of defect structures is often seriously limited by specimen noise due to contamination or oxide layers on the surfaces of a thin foil. Image simulations illustrate that, in the absence of specimen noise (under optimum conditions and subject to limitations not discussed here), a small displacement of a single atomic column can be imaged faithfully and measured directly from the image. However, the accuracy of such a measurement is compromised by specimen noise. Image simulations show the effect of specimen noise on apparent atom positions for varying amorphous surface layer thickness fraction. The present method for noise assessment is based on the average displacement of image intensity peaks due to contamination or oxide layers. To determine this average displacement, it is necessary to extract the image peak positions and compare them with a set of reference peak positions. The list of peak positions is obtained by finding the center of mass of intensity peaks located near atomic positions in the experimental image. Then a reference list is created by performing a least-squares fit of a 2D lattice upon the positions of the first list. Assuming a perfect periodic lattice, this reference list approximates the positions of intensity peaks in the absence of noise. The root mean square (rms) deviation between the lists is used as a direct measure of the noise in the image. The method described here allows a clear assessment of the specimen noise-imposed limitations to structural defect analysis in simple materials.

33469 M Yes
U. Dahmen and N. Thangaraj

Grain Boundaries in Mazed Multicrystal Microstructures of Al

6th Int'l. Conf. on Intergranular & Interphase Boundaries

Thin films of aluminum with mazed bi- and tricrystal microstructures have been produced by exploiting symmetry properties inherent in heteroepitaxial growth. These microstructures are best described as polycrystalline thin films with only two or three allowed grain orientations, rotated 90° or 30° with respect to each other. This work illustrates the unique crystallographic color symmetry and topological properties of mazed bi- and tri-crystal thin films. The faceting and atomic relaxation behavior of these films has been characterized by conventional and high resolution electron microscopy. Mazed bicrystal films have no triple junctions, and mazed tricrystal films exhibit well-controlled junctions where three identical grain boundaries meeting in a triple line. High resolution electron microscopy of significant facets, i.e. boundaries with optimum inclinations illustrates the nature of atomic relaxations in some of these grain boundaries.

33822 A No
J.O. Malm, M.A. O'Keefe

Using Convergence and Spread-of-Focus Parameters to Model Spatial and Temporal Coherence in HRTEM Image Simulations

Abstract for EMSA

In all HRTEM images, the incident electron beam suffers from the effects of limited spatial and temporal coherence. These effects produce a smearing of the image, and provide the ultimate limits as to how high a spatial frequency can be transferred to the image (i.e. resolution). The effect of partial temporal coherence is manifested as a spread of focus, and that of partial spatial coherence as incident beam convergence. The effects of partial coherence can be included in HRTEM image simulations by summing images in real space, or by applying an appropriate transmission cross-coefficient (TCC) when computing the image intensity spectrum in reciprocal space. For linear images (from specimens thin enough to behave as weak phase objects), the TCC can be simplified and described in terms of "damping envelope" functions that multiply the usual phase-contrast transfer function. Several expressions for top-hat and gaussian models of convergence damping envelopes exist in the literature and in simulation programs. The standard deviations used to compute resolution damping can thus range over a factor of more than two for the same value of convergence. Results illustrate how differences in TCCs, and thus simulated images, can arise.

33823 A No
M.A. O'Keefe and V. Radmilovic

The Effects of Small Crystal Tilts on Dynamical Scattering: Why Simulated Images are Thinner Than Experimental Ones

Abstract for EMSA

High-resolution transmission electron microscope image simulation can accurately reproduce experimental HRTEM images only when imaging parameters are accurately known. These parameters include specimen properties such as unit cell structure, crystal orientation, and specimen thickness, as well as microscope parameters such as beam energy and coherence, objective aperture size, defocus and spherical aberration. Of these parameters, the most difficult to measure, and thus to include accurately, is the specimen thickness. In many investigations specimen thickness is treated as a disposable parameter; i.e. the experimental specimen thickness is not measured, but judged to be the thickness that was used in the simulation program to produce the matching simulated image. Such a procedure can be dangerous, because image character is not unique; i.e. the same image occurs at a different thickness if other conditions are allowed to vary within experimental error. For tilted crystals, images from thinner areas will retain the correct symmetry in first order. Small tilts decrease the rate of image change with thickness, and can extend the range of thicknesses over which a "good" (thin-crystal) image can be obtained (and may unknowingly be selected for this reason -- crystallographic image processing often confirms the presence of small tilts in HRTEM images). The proportion of second-order contributions is lower from a tilted specimen, and the image appears to come from a thinner crystal. This effect is illustrated for aluminum in [001] orientation. Interestingly, the simulations show no significant effect for 1 milliradian tilt (although the peak potential drops from 106 to 99 volts); this means that normal beam convergences (usually near 1 mrad) need not be included in the diffraction calculation, at least up to 80Å thickness for atoms as light as aluminum.

---

un-numbered A No
R. Kilaas

Image Simulation in Electron Microscopy

Abstract for EMSA

The theoretical calculation of High Resolution Transmission Electron Microscopy (HRTEM) images has become a routine operation due largely to the existence of several commercially available computer programs. Associated with these "black box" calculations, exists a danger coming from the ease with which the programs can be used to produce images without any understanding of the underlying physical principles and approximations used in the calculations. While hopefully, the majority of users of image simulation take the care to understand the limitations of the technique, there are several basic principles that must be understood in order to use the technique within the limits of its applicability.

33829 A No

J. Turner, M.A. O'Keefe, and S. Paciornik

Image Processing to Extract Line Information from Micrographs

Abstract for EMSA

In processing microscope images, it is sometimes important to be able to extract the lengths and directions of linear features. For example, in characterizing transmission electron microscope images of faceted grain boundaries, the desired information is the length of grain boundary lying along each direction. In order to measure grain boundary lengths automatically, micrographs must be digitized and the linear features (e.g. the grain boundaries) binarized and reduced to a single pixel width. Then the problem requires finding two simple parameters for each line in the image: its direction and number of pixels. A new approach to this problem is to project the intensities of the source image in all possible directions, and to collect the projection results into a new two-dimensional "image" with one dimension representing the projection direction. This new image is called the sinogram of the source image. Each peak in the sino-gram represents a line, with one coordinate of the peak equal to the line's angle, and the other to its position. Intensities of peaks in the sinogram are equal to the numbers of pixels in the equivalent lines. The algorithm for the sinogram of an nxn (square) binary image over 2n angles was written as a library function in the image processing program Semper. This method produced a length error of less than 8%; angular error is less than 0.3° for all lines longer than 50 pixels.

33501 M No

H.-R. Wenk, K.H. Downing, H. Meisheng, and M.A. O'Keefe

3D Structure Determination from Electron Microscope Images: Electron Crystallography of Staurolite

Acta Cryst., A48, p.700 (1992).

Resolution of better than 2Å has been obtained in many crystals by high resolution electron microscopy. Structures are traditionally interpreted by comparing experimental images with contrast calculations. A drawback of this method is that images are 2d projections in which information is invariably lost. We have been using 3d electron crystallography, developed by biophysicists to study proteins, to investigate the crystal structure of staurolite. Amplitudes and phases of structure factors are obtained experimentally from high resolution images (Jeol ARM 1000 at the National Center for Electron Microscopy at LBL), taken in different directions. From images in five orientations we construct a 3d electron potential map with a resolution of better than 1.4Å which resolves clearly all cations (Al,Si,Fe, including those with partial occupancy) and all oxygens. We see great potential in this method for crystal structure determinations of small domains in heterogeneous crystals which are inaccessible to x-ray analysis. It is estimated that 3d structure determinations should be possible on small domains only about 10 unit cells wide and should resolve not only atom positions but also site occupancies.

---

unnumbered M R
G. Thomas

Electron Microscopy and Materials Science

Acta Microsc., Vol. 1, #1, p.1 (1992).

This paper provides a brief review of some significant aspects associated with electron microscopy and microanalysis that have become an integral part of the field of materials science and engineering. Since modern instruments provide specific and localized information on structure, morphology and chemical composition at high spatial resolutions, it is now possible to carry out the very detailed characterization necessary to establish the links between materials processing, microstructure evolution, properties and performance.

30047 M R
N. Kijima, R. Gronsky, H. Endo, Y. Oguri, S.K. McKernan, and A. Zettl

Microstructure of the High T_c Phase (T_c ~111K) in the Sb-Pb-Bi-Sr-Ca-Cu-O System

Appl. Phys. Lett., 58, 2, p.188 (1991).

The microstructure of the high T_c phase (T_c ~111K) in the Sb-Pb-Bi-Sr-Ca-Cu-O system has been determined using transmission electron microscopy. The high T_c phase has a modulated structure with b-axis wavelengths 26.9 and 36.1Å. Stacking faults along the c axis in the high T_c phase are much less numerous than in the Bi-Sr-Ca-Cu-O system, but comparable to the Pb-Bi-Sr-Ca-Cu-O system. Sb substitution for Ca may affect the internal strain of the crystal.

29285 M No

N. Kijima, R. Gronsky, S. McKennan, A. Zettl, H. Endo, and Y. Oguri

Influence of Sb Substitution for Ca to Superconductivity and Microstructure of the High-T_c Phase (T_c ~111K) in the Sb-Pb-Bi-Sr-Ca-Cu-O System

Appl. Phys. Lett., 58, 2 (1991).

A high-T_c phase with a critical temperature of 111K in the Sb-Pb-Bi-Sr-Ca-Cu-O system has been synthesized by means of a long firing period. This critical temperature is 4K higher than that of the high-T_c phase in the Pb-Bi-Sr-Ca-Cu-O system. The average chemical composition of the high-T_c phase (T_c ~111K) is 4.3%, 2.6%, 19.2%, 21.4%, 15.8% and 36.9% for Sb, Pb, Bi, Sr, Ca and Cu, respectively.

29667 M R

M.E. Tidjani, R. Gronsky, J.J. Kingston, F.C. Wellstood, and J. Clarke

Heteroepitaxial $YBa_2Cu_3O_{7-x}$-$SrTiO_3$-$YBa_2Cu_3O_{7-x}$ Trilayers Examined by Transmission Electron Microscopy

Appl. Phys. Lett., 58, 7, p.765 (1991).

We report high-resolution transmission electron microscopy and electron diffraction studies of the heteroepitaxial superconductor-insulator- superconductor system $YBa_2Cu_3O_{7-x}$-$SrTiO_3$-$YBa_2Cu_3O_{7-x}$ deposited on polished (001) MgO substrates by in situ laser ablation. The resulting films grow epitaxially and consistently preserve a parallel orientation between the close-packed (001) $YBa_2Cu_3O_{7-x}$ planes and (001) $SrTiO_3$ planes over the entire trilayer, even in the presence of ledges or steps along vicinal interfaces. Although the interface regions showed strain occasionally relieved by stacking faults, they were free of disorder and any evidence of impurity phases. The observed epitaxial growth is very likely responsible for the excellent electrical properties found in similarly constructed multilayer interconnects.

30397 M R
K. Krishnan

Structure of a Newly Synthesized BC_3 Films

Appl. Phys. Lett., 58, p.1857 (1991).

We have measured the electron energy-loss spectrum (EELS) of BC_3 at sub-eV resolution. Important differences between the total density of states of BC_3 at the threshold of the K edge, predicted by earlier ab initio calculations, have been observed. We conclude from our measurements that the atomic arrangement in these materials can be described as graphite sheets with B replacing every third C atom. We suggest that further understanding of the electronic structure of BC_3, can be derived by comparing such EELS data with calculations of the local density of states of bulk BC_3 and including interlayer interaction.

30558 M No
M. Salvadori, J. Ager, I. Brown, and K. Krishnan

Diamond Synthesis by Microwave Plasma Chemical Vapor Deposition Using Graphite as the Carbon Source

Appl. Phys. Letts., 59, p.2386 (1991).

We report on the growth of high quality diamond using a microwave plasma chemical vapor deposition (CVD) system in which the feed gas contains no hydrocarbons, but instead the source of carbon is a graphite piece which resides within the plasma volume. Results of experiments using this technique by itself and in combination with the normal methane feed gas method are described. Diamond grown in this way was found to be particularly pure and of high crystallinity.

30128 M R

K.M. Krishnan, E.S. Menon, P. Huang, P.P. Singh, and D. de Fontaine

Short Range Order Effects on Copper $L_{3,2}$Transitions in Cu-Pd Alloys

Appl. Phys. Lett., 60 (14) p.1762 (1992).

The unoccupied *d*-electron density of states of a range of $Cu_{1-x}Pd_x$ (x = 0-0.35) alloys, based on measurements of copper $L_{3,2}$ transitions in electron energy-loss spectroscopy, is shown to be critically dependent on short-range order. This finding is supported by band structure calculations where the *d*-hole count at the Cu site for disordered alloys is found to be independent of the composition. Based on the above, a linear correlation between the degree of short-range order, as defined by the splitting of the diffuse maxima in the diffraction patterns, and the *d*-band occupancy has been established.

33506 M No

A. Claverie, K. Yu, W. Swider, Z. Liliental-Weber, M.A. O'Keefe, R. Kilaas, J. Pamulapati, and P. Bhattacharya

Structural Characterization of Low Temperature Molecular Beam Epitaxial $In_{0.52}Al_{0.48}$ As/InP Heterolayers

Appl. Phys. Letts. 60, 8, p.989 (1992).

A systematic study of the structural quality and arsenic content of as-grown $In_{0.52}Al_{0.48}$ As/InP layers deposited on InP by molecular beam epitaxy at temperatures between 150 and 450° C was performed using transmission electron microscopy and particle-induced x-ray emission. We found that the amount of As incorporated in the layers generally increases with decreasing growth temperature, with the crystalline quality of the layers being good at growth temperatures higher than 200° C. At 150° C, a large density of pyramidal defects is formed, the defects are related to the very large amount of excess As incorporated into the layer. The mechanism leading to the formation of these defects are discussed. At 200° C however, the amount of excess As is lower than expected, and wavy streaks of diffuse scattering are seen in electron diffraction. It is shown that small ordered domains of the CuPt type on the group III atoms are responsible for these features.

31300 M P
N. Cho, K. Krishnan, C. Lee, and R. Farrow

Twin Formation in Ag Seeded Co/Pt Multilayers Grown on GaAs by Molecular Beam Epitaxy

Appl. Phys. Letts., 60, p.2371 (1992).

Molecular beam epitaxy was used to grow ultrathin Co-Pt multilayers on GaAs (111) substrates with 200 Å thick Ag layer as a buffer. Magnetic properties (B-H loop) of the multilayers, measured by a vibrating sample magnetometer, confirmed that these samples exhibit strong anisotropy perpendicular to the film surface. Reflection high energy electron diffraction and low-energy electron diffraction showed that twin-related Ag grains nucleated on the substrates. The epitaxial relationship of the multilayers with respect to the substrate was investigated by high resolution transmission electron microscopy. Twin related grains, 30-40 nm in diameter, are present in the multilayers. These twins are generated either by propagation of existing twin boundaries in the Ag layer into the multilayers or by nucleation of twin-related Pt grains on the Ag buffer surface.

31295 M No
C. Lucas, and D. Loretto

New Insight into the Structure and Growth of CaF_2/Si(111)

Applied Phys. Letters, Vol. 60, p.2071 (1992).

We have used transmission electron microscopy and x-ray crystal truncation rod measurements to investigate thin (<50 Å) CaF_2 films grown on Si(111) substrates by molecular beam epitaxy. The results indicate that CaF_2/Si can be structurally as perfect as $NiSi_2$/Si and $CoSi_2$/Si, and enable a better understanding of the interface structure.

32191 M RP
N. Thangaraj, K.H. Westmacott, and U. Dahmen

Epitaxial Growth of (001) Al on (111) Si by Vapor Deposition

Applied Phys. Lett., 61, #8, p.913 (1992).

Heteroepitaxial growth of (001) Al thin films on Si (111) single crystal substrates by vapor deposition was studied by means of x-ray diffraction (XRD), Rutherford back scattering (RBS) spectrometry and transmission electron microscopy (TEM) techniques. It was observed that the films deposited at room temperature exhibit random (111) texture, while the films deposited at 280° C show perfect epitaxial alignment of (001) Al planes with (111) Si planes. In the interface plane <110> close packed directions in both the film and the substrate are parallel and hence Al grows with three orientation variants in a unique mazed tricrystal arrangement.

32197 M PR
N. Thangaraj, K.H. Westmacott, and U. Dahmen

Epitaxial Growth of (011) Al on (100) Si by Vapor Deposition

Applied Physics Lett., 61, 1, p.37 (1992).

The morphology, orientation relationship and interface structure of Al vapor deposited on (100) Si single-crystal substrates were investigated by x-ray diffraction and transmission electron microscopy. It was shown that vapor growth at room temperature results in a random (111) texture, whereas growth at 280° C leads to films with high-quality (011) epitaxy and a high degree of grain boundary faceting. Due to alignment of close-packed directions in the plane of the interface there are two orientation variants with a morphology characterized by an oriented 90° (011) mazed bicrystal structure.

32360 M PR
K.M. Krishnan

Ferromagnetic δ-$Mn_{1-x}Ga_x$ Thin Films with Perpendicular Anisotropy

Applied Physics Letters, 61, (19), p.2365 (1992).

We report the structure and properties of the thermodynamically stable δ-phase $Mn_{1-x}Ga_x$ thin films on GaAs. X-ray Θ-2Θ scans and grazing incident scattering measurements confirmed that the unit cell of this phase is tetragonal (a = 0.279 nm, c = 0.351nm) and grows with the c-axis oriented normal to the (001) GaAs substrate surface. X-ray emission spectroscopy confirmed the composition to be 62 ± 2% Mn. Polar Kerr rotation, SQUID and vibrating sample magnetometer measurements with the field applied along the thin film normal showed nearly perfect square hysteresis loops confirming perpendicular anisotropy of the films. The film exhibits a Kerr rotation angle of ~0.1° at 820 nm, a coercivity of 6.27 kOe and a saturation magnetization of 460 emu/cm3. The optical reflectivity of the film was 65-70% over a broad range of wavelengths. This unique set of properties make it a very promising material for magneto-optic recording with the additional potential of integrating semiconductor/magnetic devices by suitable patterning techniques.

33539 M No
M.A. Brewer, and K. Krishnan

Effects of Substrate Surface Preparation on Diamond Nucleation in Chemical Vapor Deposition

Applied Physics Letters, (submitted, 1993).

Microwave plasma CVD diamond was deposited on silicon substrates with different surface preparations to evaluate the parameters that affect nucleation density and quality. (100) silicon wafers were polished or randomly distributed with 1-μm diamond, 0.2-μm SiC or 0.8-μm Si_3N_4 and the resulting nucleation density after 60-min. depositions compared. Diamond resulted in the best nucleation enhancement, then Si_3N_4 and SiC, respectively. Given that SiC was found to be an interfacial layer between silicon and diamond films by some experimenters, it was surprising that SiC particles did not nucleate diamond. Other silicon substrates were scratched with a tungsten scribe to create surface defects without leaving residual powder particles. Nucleation was not enhanced on these substrates. These measurements support an earlier result that diamond nanocrystallites embedded in the substrate during its preparation are the preferred sites for nucleation.

33574 M No

S. Im, J. Washburn, R. Gronsky, N.W. Cheung, and K.M. Yu

Defect Control During Solid Phase Epitaxial Growth of SiGe Alloy Layers

Applied Physics Letters (submitted 1/298/93).

A systematic study of the processing procedures required for minimizing structural defects generated during the solid phase epitaxial (SPE) growth of SiGe alloy layers is described. It includes high dose Ge implantation into Si at liquid nitrogen temperature (LNT), sequential carbon implantation, and an 800° C anneal. The LNT implantation step considerably reduces the density of end-of-range (EOR) defects relative to that found in SPE grown SiGe layers implanted at room temperature, while the sequential implantation of carbon ions before annealing effectively suppresses the formation of stacking faults that are found to form at a threshold peak concentration of about 6 at %Ge in the absence of carbon.

32125 M R

R. Jelinek, B.F. Chmelka, Y. Wau, M.E.. Davis, J.G. Ulan, R. Gronsky, and A. Pines

Adsorption Effects in Aluminophosphate Molecular Sieves Studied by Al Double-Rotation NMR

Catalysis Letters, 15, p.65 (1992).

Al double rotation NMR (DOR) spectroscopy is used to investigate structural changes in the framework of several aluminophosphate molecular sieves upon adsorption of water. The shapes, widths, and positions of the spectral lines yield information on the aluminum environments, adsorption sites, and degree of structural disorder undergone upon water adsorption.

30365 M P
U. Dahmen

Characterization of Crystalline Interfaces by Advanced Electron Microscopy

Crystalline Interfaces Workshop

Notes from the discussions at an international workshop on the Characterization of Crystalline Interface by Advanced Electron Microscopy held at the National Center for Electron Microscopy in August, 1990.

UCRL111359 M No
A.J. Schwartz and L.E. Tanner

HRTEM Observations of Modulated Structures in Ti-Pd-Cr-β_2 Alloys

ICOMAT 92

Conventional and high resolution transmission electron microscopy (HRTEM) and electron diffraction (ED) have been used to examine a series of $Ti_{50}Pd_{50-x}Cr_x\beta_2$ (B2,CsCl-type crystal structure) alloys with x between 6 and 10 at .% in order to determine the nature of the modulated structures that develop on cooling. The ED and HRTEM results reveal that the modulation periodicity (inverse of the satellite spacing) varies from three $(110)_{B2}$ planes in the 6 at .% Cr alloy to four $[110]_{B2}$ planes for the 10 at .% Cr alloy. Over the same composition range, the "monoclinic angle" (defined between $(200)_{B2}$ and $(020)_{B2}$ reflections) is found to increase linearly from 88 to 90°. It is suggested that these effects are associated with the substitution of Cr for Pd that gives rise to an electronically driven $(110)_q(110)_\epsilon$ phonon anomaly.

29967 M No
M. Witcomb, and U. Dahmen

A Jet Polishing Technique for Thinning Two Phase Materials

EMSSA Vol. 20, p.9 (1991).

A common problem in the preparation of thin foils for transmission electron microscopy is the different thinning rate in two-phase materials. Often this leads to foils in which the majority (matrix) phase is evenly polished, while the minority (precipitate) phase is either etched out or stands proud of the surrounding material. In this report we describe a two-stage jet polishing technique that has been used successfully on different relatively coarse two-phase structures.

---

un-numbered M No
J.B. Liu, and R. Gronsky

Isolation of a Failed Transistor for TEM Sample Preparation

Int'l. Conf. on Electron Microscopy

Modern troubleshooting and diagnostics in the semiconductor industry requires that TEM analysis be done directly on the cross section along the desired direction of the failed transistor that is identified by electronics testing. Many previous studies have been conducted for this purpose: cross sectional TEM sample preparation by mechanical polishing using a tripod polisher, and a selected-area modification of the technique for improved precision. In this paper, the method used to track the failed transistor is described in detail.

---

unnumbered M No
D. Carl, D. Hess, M. Lieberman, T. Nguyen, and R. Gronsky

Effects of dc Bias on the Kinetics and Electrical Properties of Silicon Dioxide Grown in an Electron Cyclotron Resonance Plasma

J. Appl. Phys, 70, p.1 (1991)

Thin (3-300 nm) oxides were grown on single-crystal silicon substrates at temperatures.from 523 to 673 K in a low-pressure electron cyclotron resonance (ECR) oxygen plasma. Oxides were grown under floating, anodic or cathodic bias conditions, although only the oxides grown under floating or anodic bias conditions are acceptable for use as gate dielectrics in metal-oxide-semiconductor technology. Oxide thickness uniformity as measured by ellipsometry decreased with increasing oxidation time for all bias conditions.

---

unnumbered M No
S.E. Fendorf, M. Fendorf, R. Gronsky and D.L. Sparks

Inhibitory Mechanisms of Cr(III) Oxidation by MnO_2

J. Colloid & Interf. Sci., Vol. 153, # 1, p.37 (1992).

The oxidation of Cr(III) by Mn-oxides is inhibited at pH values greater than 4. In this paper, we show that the inhibition is due to the formation of a $Cr(OH)_3$ precipitate on δ-MnO_2. Subsequent to a monolayer of Cr(III) oxidation, surface facilitated nucleation of $Cr(OH)_3$ terminates the redox reaction between Mn(IV)/Mn(III) and Cr(III). The Cr(OH)3 phase acts both as a barrier to electron transfer between solution Cr(III) species and Mn(IV)/Mn(III), and as a redox stable sink for Cr(III). This system imposes some unique boundaries on surface precipitation as direct surface complexation of Cr(III) would result in an electron transfer between Cr(III) and Mn(IV)/Mn(III). Therefore, the electrostatic influence of the surface appears to promote the nucleation of this hydrolyzable metal ion without direct surface complexation.

---

unnumbered M No
S.E. Fendorf, M. Fendorf, R. Gronsky and D.L. Sparks

Surface Precipitation Reactions on Oxide Surfaces

J. Colloid & Interf. Sci., 148, p.295 (1991).

Retention of heavy metal ions on solid surfaces is an important process for many catalytic and electrochemical reactions, and for maintaining environmental quality. Determining reaction mechanisms are essential for understanding such processes. However, various mechanisms have been proposed for the sorption of cationic heavy transmission electron microscopy (HRTEM) for the formation of a surface precipitate prior to bulk solution precipitation. Furthermore, the type of surface present influenced the onset of surface precipitation. At pH 5 and 400 mM Al(III), a surface precipitate was observed on MnO_2 (the birnessite phase), but was not apparent on TiO_2 (the rutile phase). Thus, surface precipitation reactions must be considered in modeling the sorption mechanisms of hydrolyzable metal ions on oxide surfaces. In addition, surface precipitates will alter the characteristics of the surface; beyond complete coverage the resulting colloid will exhibit the properties of the metal hydroxide surface precipitate.

---

unnumbered M No
T. Epicier, G. Thomas, H. Wohlfromm, and J. Moya

High Resolution Electron Microscopy Study of the Cationic Disorder in Al_2TiO_5

J. Mat. Res., Vol. 6, #1, p.138 (1991).

As part of a research program devoted to the microstructural characterization of Al_2TiO_5-based compounds, high resolution electron microscopy (HREM) has been undertaken in order to study the crystallographic arrangement, especially ordering possibilities, of Al and Ti cations in the metallic sublattice of aluminum titanate. It is seen that adequate experimental conditions, mainly defocus setting, for a resolution of at least 2.5 Å point-to-point, enable the disordered model to be directly and unambiguously proved on [100]-oriented micrographs.

30765 M R
M. Carey, F. Spada, A. Berkowitz, W. Cao, and G. Thomas

Preparation and Structural Characterization of Sputtered CoO, NiO and $Ni_{0.5}Co_{0.50}$ Thin Epitaxial Films

J. Mat. Res., Vol. 6, 12, p.2680 (1991).

Single phase CoO, NiO, and $Ni_{0.5}Co_{0.50}$ epitaxial films have been prepared by reactive sputtering onto (0001) α-Al_2O_3 substrates maintained at 373 K. Epitaxy was confirmed by x-ray diffraction (XRD) and high resolution electron microscopy (HREM) techniques. XRD experiments indicate that these monoxide films are cubic and contain rotation twins with the twin axis parallel to (111). Lattice parameters for the CoO and NiO films are 0.4254 ± 0.0001 nm and 0.4173 ± 0.0006 nm respectively, and agree with published values for the corresponding bulk oxides.

---

unnumbered M No
M. Libera, M. Chen, and K. Rubin

Germanium Supersaturation During the Crystallization of Amorphous Te-Ge-Sn Thin Films

J. of Mat. Res., 6, p.2666 (1991).

The structure and phase relations of Te-Ge-Sn thin films are examined with application to erasable optical storage media. Free energy data from the literature predict that the region of the Te-Ge-Sn phase diagram between Ge, Sn, and the TeGe-TeSn psuedobinary consists of one two-phase field (α-Ge and $Te_{50}(Ge_xSn_{1-x})_{50}$) and one three-phase field (α-Ge, β-Sn, and TeSn). Electron diffraction from five different Te-Ge-Sn films annealed at 623K experimentally confirms this prediction. Of particular significance is that laser-induced crystallization produces a single-phase structure consisting of the Te-Ge-Sn compound phase which is supersaturated with respect to the excess Ge. This supersaturation leads to a disordering of the equilibrium NaCl-type structure of this phase.

33607 M No
J.B. Liu, B.M. Tracy, and R. Gronsky

Selected Area Polishing for Precision TEM Sample Preparation

J. Microscopy Tech. (submitted, 1993).

A selected area mechanical polishing technique has been developed to improve the precision of cross-sectional TEM sample preparation, based upon the early work of Benedict et al. (1990). TEM samples were made from a preselected section through the middle of a 1 μm wide band of transistors extending laterally for more than 1 mm by precise control over the plane of polish with a corresponding reduction in sample preparation time. To illustrate the application of this technique, a uniformly-thin, electron transparent TEM sample of a single, specific, failed transistor is obtained from a 4 mm by 10 mm device array.

---

un-numbered M No
W.W. Milligan, S.A. Hackney, M. Ke and E.C. Aifantis

In Situ Studies of Deformation and Fracture in Nanophase Materials

J. of Nanostructural Materials

Nanocrystalline gold (8-25 nm grain size) and gold/silicon nanocomposites were prepared by sputtering and then strained to fracture in a transmission electron microscope. *In situ* and *post mortem* analyses revealed that the nanophase gold films were ductile, and significant plasticity was associated with fracture. Observations of pore formation, as well as a strain-rate effect on deformation behavior and direct lattice imaging of deformation, all indicated that the deformation occurred by diffusion-based mechanisms. Fracture was intergranular, but not brittle. Gold/silicon nanocomposites containing large volume fractions of brittle, amorphous Si and nanocrystalline gold precipitates exhibited behavior indicating significant toughness.

---

un-numbered M No
J. Liu, M.L. Dass, and R. Gronsky

Transmission Electron Microscopy Study of Two Dimensional Semiconductor Device Junction Delineation by Chemical Etching

J. Vacuum Sci. & Tech. (accepted, 1993).

Quantitative chemical delineation of both n+ and p+ junctions in silicon-based integrated circuits has been achieved and monitored with respect to etching time, temperature, and ultraviolet illumination, using samples prepared by a new planar polishing technique for uniform initial flatness. Junction depths and dopant profiles obtained from cross-sectional transmission electron microscopy images are compared and cross-calibrated with both secondary ion mass spectrometry and spreading resistance profiling, confirming that dopant concentrations of 10^{17} cm^{-3} are detected and laterally mapped with better than 10 nm spatial resolution.

29881 M R
N. Kijima, and R. Gronsky

Crystal Structure of the High-Tc Phase (T_c~111K) in the Sb-Pb-Bi-Sr-Ca-Cu-O System

Jap. J. of Appl. Phys., Vol. 31, p.L82 (1992).

The crystal structure of the high-T_c phase (T_c~111K) in the Sb-Pb-Bi-Sr-Ca-Cu-O System has been determined using transmission electron microscopy. Both energy dispersive x-ray spectroscopy and high-resolution transmission electron microscopy HRTEM) indicate that Sb partially substitutes for Ca in the high-T_c phase (T_c~111K) of the Sb-Pb-Bi-Sr-Ca-Cu-O system, accompanied by extra oxygen atoms that compensate the oxygen deficiency in the central Cu-O layer sandwiched between adjacent Ca/Sb layers.

30049 M R

N. Kijima, R. Gronsky, H. Endo, Y. Oguri, S.K. McKernan and A. Zettl

Superconductivity and Chemical Composition of the High-T_c Phase (T_c~111K) in the Sb-Pb-Bi-Sr-Ca-Cu-O System

Jap. J. of Appl. Phys., Vol. 30, #1B, p.L99 (1991).

A superconducting phase with a critical temperature of 111K in the Sb-Pb-Sr-Ca-Cu-O system has been synthesized by means of a long firing period. Its crystal structure is similar to the high-T_c phase (107 K) in the Pb-Bi-Sr-Ca-Cu-O system, and its average chemical composition is 4.3%, 2.6%, 19.2%, 21.4%, 15.8% and 36.9% for Sb, Pb, Bi, Sr, Ca and Cu, respectively. The summation of the Sb concentration and the Ca concentration is approximately the same for all the samples of this phase, implying that Sb substitutes for Ca, and oxygen atoms are introduced to compensate the oxygen deficiency in the central Cu-O layer sandwiched by the two Ca layers in the crystal structure of the High-T_c phase.

29989 M R

M. Salvadori, M. Brewer, J. Agar, I. Brown, and K. Krishnan

Effect of a Graphite Holder on Diamond Synthesis by Microwave Plasma Chemical Vapor Deposition

Journal Electrochemical Soc., Vol. 139, #2, p.588 (1992).

A microwave plasma chemical vapor deposition system using a graphite retaining ring as the sample holder has been used for low pressure diamond synthesis. The hydrogen plasma in this system can etch material from the graphite surface. By conditioning the surface of the graphite ring, this process can be reversed, and material can then be deposited onto the graphite surface by the plasma, rather than being etched from it. The result of conditioning the graphite retaining ring was to cover the graphite with diamond, and hinder plasma etching of carbon from the retaining ring. The samples were characterized using Raman Spectroscopy and Scanning Electron Microscopy, and the surface of the retaining ring was also studied with Raman.

32202 M RP
N.-H. Cho, K.M. Krishnan, C.A. Lucas, and R.F. Farrow

Microstructure and Magnetic Anisotrophy of Ultrathin Co/Pt Multilayers Grown on GaAs (III) by MBE

Journal of Applied Physics, 72, #12, p.5799 (1992).

Multilayers of $[Co_{3Å}, Pt_{15Å}]_x$, x = 15 or 30 repeats, with or without a 200Å silver buffer layer, were grown on GaAs (III) substrates by molecular beam Epitaxy (MBE). Vibrating sample magnetometry (VSM) measurements confirmed that the samples with the Ag buffer layer show strong uniaxial magnetic anisotropy perpendicular to the surface. The perpendicular anisotropy exhibited by these metallic superlattices is discussed in terms of the microstructure of the overall multilayer stack, as well as the structural characteristics of the Co interface layer. Samples grown on the Ag buffer layer show strong (111) texture with 30-40 nm size twin-related grains. These grains correspond to the two possible (111) results in randomly oriented 10-20 nm grains. All samples exhibit a repeat period of 1.83 nm in both low-angle reflectivity and high-angle Θ-2Θ x-ray scattering measurements. In addition, transverse scans through the low-angle multilayer Bragg peaks show the interfaces to be diffuse in nature, indicative of considerable in-plane inhomogeneity and/or compound formation. High-resolution electron microscopy measurements of cross sections compared with image simulations confirm that the interface layer is diffuse and its stoichiometry is such that the Co occupation is less than 40%. Redistribution of Co should then extend over at least four monolayers. The nanostructure of the samples grown with the Ag buffer layer comprises an eight atomic layer repeat with the Co interface layer diffuse over four monolayers. The microstructure is strongly (111) textured with columns of twin related 30 nm sized grains separated by a 1 nm wide second phase. It is suggested that the combination of interdiffusion, highly oriented by twin-related columnar growth, small grain size with a possible nanometer-scale second phase may be the key to the understanding of the perpendicular anisotropy observed in these (111) superlattices.

32975 M R
W. Jolly and J. Turner

Computer Simulation of the Sabatier Effect

Journal of Image Sci. & Techn., 36, #6, p.558 (1992).

All of the features of the Sabatier solarization, including Sabatier border lines, are represented in the Sabatier H & D curve; that is, they are a consequence of the desensitization in those regions of the emulsion that received a perceptible initial exposure. This point is emphasized by showing that a computer-simulated Sabatier solarization of a black-and-white print (based on a one-to-one correspondence between a normal and Sabatier-solarized step wedge) and the actual darkroom solarization are very similar. Therefore adjacency effects, such as the Mackie line, are not importantly involved in the Sabatier effect.

32819 M P
B. Zhang, K.M. Krishnan, C.H. Lee, and R.F.C. Farrow

Magnetic Anisotropy and Lattice Strain in Co/Pt Multilayers

Journal of Applied Physics, (accepted 1992).

We report on the correlation between perpendicular anisotropy and in-plane lattice strain in Co/Pt multilayers. $(Co_x/Pt_y)n$ samples, where x, y are the thickness of the individual Co and Pt layers and n is the number of repeats were prepared by Molecular Beam Epitaxy and studied by means of polar Magneto-Optic Kerr effect and transmission electron microscopy. Kerr rotation data and electron diffraction experiments show that the largest perpendicular anisotropy and square hysteresis loop occur when x = 3Å while the Pt layers are subjected to about -2% in-plane strain. As Co thickness increases, Co and Pt layers gradually lose coherency and the magnetic anisotropy goes from perpendicular to planar. This is accompanied by a relaxation of lattice strain in both Co and Pt layers. The close relationship between magnetic anisotropy and lattice strain can be explained as magneto-elastic anisotropy or stress anisotropy effect due to lattice mismatch between the adjacent epitaxial layers.

29679 M R
N. Merk and G. Thomas

Structure and Composition Characterization of Submicronic Mullite Whiskers

Journal of Mats. Res., Vol. 6, p.825 (1991).

Two sets of submicronic mullite whiskers, which have been potential applications for fiber reinforced composites or as a thermal insulator, have been characterized to be tetragonal or orthorhombic using x-ray and electron microscopy techniques. The whiskers decompose upon heating under vacuum with a continuous loss of silicon and reduction in oxygen content up to the limit for which pure aluminum metal and alpha-alumina are formed.

33385 M No
C. Burmester, L. Wille, P. Stearne, and R. Gronsky

Long Range Interactions, Long Range Order, and a Devil's Staircase in $YBa_2Cu_3O_z$

Journal of Physics, Vol. 4, L-583 (1992).

It is shown that the oxygen ordered superstructures observed experimentally in $YBa_2Cu_3O_z$ can be understood in terms of an Ising Hamiltonian containing screened Coulomb repulsions between any two oxygen sites, augmented with a short range attractive covalent interaction between oxygen sites adjoined by a copper atoms. Spatially modulated commensurate phases separated by smooth soliton-like domain walls are obtained through Monte Carlo simulations. These simulations indicate the existence of a complete devil's staircase of phases. It is predicted that the plateau fine structure of the T_c-z curve and the bond valence sum also exhibit experimentally observable staircase behavior.

28366 M No
V. Radmilovic, G. Thomas

Microstructure of α-Al Base Matrix and SiC Particulate Composites

Mat. Sci. & Eng., A-132, p.171 (1991).

The microstructures of a high temperature monolithic Al-Fe-V-Si alloy and a metal matrix and SiC particulate composite (MMC) based on this alloy matrix were characterized by conventional and high resolution transmission electron microscopy, microdiffraction and x-ray spectroscopy techniques. Silicide particles of average composition $Al_{13}(Fe, V)_3Si$ were present in both of these materials. These particles were unstable under the electron beam at voltages above 200 kV; and exhibited radiation-induced disordering. SiC particulates present in the MMC structure were predominantly of the hexagonal 6H polytype, but the rhombohedral 87R-VII polytype was also observed. A very thin reaction layer was present between the matrix and SiC particles. No segregation of alloying elements such as iron, vanadium, or silicon at the matrix-SiC interface was observed. The second phase present at the α-Al-SiC interface was probably a disordered silicide.

---

unnumbered M No
J. Douin, T. Epicier, J.-M. Penisson and A. Thorel

High Resolution Transmission Electron Microscopy Study of Interfaces

Mat. Chem. and Physics, 32, p.77 (1992).

The study of interfaces by means of High Resolution Transmission Electron Microscopy (HRTEM) is discussed through selected observations conducted on the Atomic Resolution Microscope (NCEM, Berkeley, USA). The precipitation of germanium into aluminum, the study of interfacial non-crystalline films in silicon nitride, the determination of the chemical nature of twin planes in $CuAlO_2$, and the structure of the $\varepsilon 3$ grain-boundary in aluminum are the examples that serve to illustrate problems of relevance in the atomistic study of interface with HRTEM.

22889 M R
C.F. Willis, R. Gronsky, and T.M. Devine

Carbide Precipitation in Welds of Two-Phase Austenitic-Ferritic Stainless Steel

Met. Trans. A, Vol. 22A, p.2889 (1991).

Transmission electron microscopy (TEM) and microanalytical chemistry were performed on sensitized samples of duplex welds that exhibited both skeletal ferrite microstructures and lath ferrite microstructures. The objective was to understand why welds with lath ferrite, contrary to a theoretical prediction, are not immune to sensitization. Most of the ferrite austenite (α–γ) interphase boundaries in the welds with skeletal ferrite were curved and incoherent, while those in welds with lath ferrite, were predominantly planar and semicoherent. The density of carbide precipitation on incoherent boundaries was much greater than that on semicoherent boundaries. Carbide precipitates on incoherent boundaries were typically equiaxed, while those on semi-coherent boundaries had very high aspect ratios and appeared to form along ledges in the inter-phase boundary. During sensitizing heat treatments, the chromium-depleted zone on the ferrite side of the interphase region transformed to austenite, causing the α–γ interphase boundary to move into the ferrite region.

30917 I, M R
U. Dahmen

TEM Analysis of Crystalline Interface Structure: The State of the Art

Microbeam Analysis, #10, p.205 (1991).

The characterization of the structure and chemistry of solid/solid interfaces is becoming increasingly important in materials science. Although electron microscopy has contributed a great deal to our present understanding of interfaces, many problems remain to be solved. A recent workshop held at the National Center for Electron Microscopy in Berkeley examined the field in some detail with the goal of pinpointing the most important problems, present limitations, and future developments. This paper will present a selective illustrative summary of the field on the basis of this workshop.

---

unnumbered M R
D.F. Blake, F. Freund, K.M. Krishnan, C.J. Echer, R. Shipp, T.T. Bunch, A.G. Tielens, R.J. Lipari, C.J. Hetherington, and S. Chang

The Nature and Origin of Interstellar Diamond

Nature, Vol. 32, #6165, p.611 (4/88).

Microscopic diamond was recently discovered in oxidized acid residues from several carbonaceous chondrite meteorites (for example, the Cδ component of the Allende Meteorite). Some of the reported properties of Cδ seem in conflict with those expected of diamond. Here we present high spatial resolution analytical data which may help to explain such results. The Cδ diamond is an extremely fine-grained (0.5-10 nm) single-phase material, but surface and interfacial carbon atoms, which may comprise as much as 25% of the total, impart an 'amorphous' character to some spectral data. These data support the proposed high-pressure conversion of amorphous carbon and graphite into diamonds due to grain-grain collisions in the interstellar medium although a low pressure mechanism of formation cannot be ruled out.

---

unnumbered M No
N. Kijima and R. Gronsky

Crystal Structures of Iodine Intercalated Superconductors in the I-Bi-Sr-Ca-Cu-O System

Mitsubishi Kasei R&D Review, 6, #2, p.58 (1992).

The crystal structures of stage-n iodine-intercalated superconducting $IBi_{2n}Sr_{2n}Ca_nCu_{2n}O_x$ have been determined by transmission electron microscopy (TEM) to belong to the space group Pma2 with $a = 5.4Å$, $b = 5.4Å$, and $c = 3.6 + 15.3\ n$ Å when stage number n is odd, and Bbmb with $a = 5.4Å$, $b = 5.4Å$, and $c = 2(3.6 + 15.3\ n)$ Å when n is even. Iodine atoms intercalated between Bi-O bilayers expand the distance between the Bi-O layers by 3.6Å and alter the atomic stacking across Bi-O layers from the staggered configuration characteristic of host superconducting $Bi_2Sr_2CaCu_2O_x$ to a vertically aligned configuration. A comparison of the superconducting transition temperatures of the host material and iodine-intercalated superconductors of different stages suggests that the coupling between each pair of adjacent blocks contributes 5 K to T_c in $Bi_2Sr_2CaCu_2O_x$.

---

unnumbered M No
W. Dong, T. Baird, J.R. Fryer, C.J. Gilmore, D.D. MacNicol, G. Bricogne, D.J. Smith, M.A. O'Keefe, and S. Hovmöller

Electron Microscopy at 1-Å Resolution by Entropy Maximization and Likelihood Ranking

Nature, Vol. 355, 2/13/92.

The resolution of electron microscopy may be extended by combining the phase information in microscope images with electron diffraction intensities. A general method for obtaining structural reconstructions at a resolution greater than that of the phase information is demonstrated for crystals of perchlorocoronene. By using entropy maximization methods combined with likelihood ranking the resolution is extended from 0.32 nm in the microscope images to 0.1 nm in the reconstruction from phase and intensity data.

---

unnumbered M No
E.S. Menon, and K.M. Krishnan

Charge Transfer and Short-Range Order in Cu-Pd and Ni-Mo Alloys

Phil. Mag. Lett., Vol. 66, #5, p.271 (1992).

Water-quenched samples of Cu-Pd and Ni-Mo alloys have been studied by electron diffraction and electron-energy-loss spectroscopy. Diffraction patterns from these alloys exhibit pronounced diffuse scattering due to short-range order. Determination of the white-line intensity in the energy-loss spectra from these samples indicated a concentration dependence and the results are discussed in terms of charge transfer associated with short-range order.

29843Rev M R
M.E. Tidjani, and R. Gronsky

Structural Characterization of the Ag-$YBa_2Cu_3O_{7-x}$ Interface

Physica C, 191, p.268 (1992).

Silver contacts to the high critical temperature (T_c) superconductor $YBa_2Cu_3O_{7-x}$ (YBCO) are characterized using high resolution transmission electron microscopy (HRTEM). Observations of the interfacial regions reveal that Ag bonds to YBCO without any intermediate phase formation but with a preferred orientation relationship, in which the close packed planes and directions of the metal are parallel to those of the superconductor. The formation of $(111)_{Ag}$ interfaces and facets are also strongly favored during deposition. The as-deposited Ag film exhibits a granular morphology and a high twin density, especially when the surface of YBCO is corrugated and structurally unstable. Annealing of the Ag-YBCO interface results in measurable grain growth and a decrease in the density of structural defects within the deposited Ag. At regions where the surface of YCO is not flat, however, there is precipitation of isolated Ag-bearing particles.

---

unnumbered M No
C.A. Lucas, G.C.L. Wong, and D. Loretto

Structural Transitions of the CaF_2/Si(111) Interface

Phys. Rev. Lett., (accepted, 1992).

We have used x-ray reflectivity and transmission electron microscopy to study the CaF_2/Si(111) interface. The results are consistent with a reconstructed two-layer CaF interface which can be irreversibly transformed to a different structure simply by increasing the thickness of the CaF_2 overlayer. We are able to reconcile previous measurements of the interface structure and gain insight into the rich variety of phenomena that may be observed at heteroepitaxial interfaces.

32146 M R
N. Kijima, R. Gronsky, X.D. Xiang, W.A. Vareka, J. Hou, A. Zettl, J.L. Corkill, and M.L. Cohen

Structural Properties of Stage 1 Iodine Intercalated Superconducting I $(Bi_{0.915}Pb_{0.085})_2$ $(Sr_{0.93}Pb_{0.07})_2$ $(Ca_{0.965}Pb_{0.035})_2$ Cu_3O_x

Physica C, 198, p.309 (1992).

The crystal structure of stage-1 iodine intercalated superconducting I $(Bi_{0.915}, Pb_{0.085})_2$ $(Sr_{0.93}, Pb_{0.07})_2$ $(Ca_{0.965}, Pb_{0.035})_2$ Cu_3O_x has been determined by transmission electron microscopy to belong to the space group Pma2 with lattice parameters $a = 5.4$Å, $b = 5.4$Å, and $c = 22.0$Å. Iodine atoms intercalated as monolayers between every Bi-O bilayer alter the atomic stacking across Bi-O layers from the staggered configuration characteristic of superconducting $(Bi_{0.915}, Pb_{0.085})_2$ $(Sr_{0.93}, Pb_{0.07})_2$ $(Ca_{0.965}, Pb_{0.035})_2$ Cu_3O_x to a vertically aligned configuration in I$(Bi_{0.915}, Pb_{0.085})_2$ $(Sr_{0.93}, Pb_{0.07})_2$ $(Ca_{0.965}, Pb_{0.07})_2$ u_3O_x. Iodine bilayers have also been observed to form between Bi-O layers, yielding a new series of stage-n iodine-intercalated compounds.

30948 M R

N. Kijima, R. Gronsky, X. Xiang, W. Vareka, A. Zettl, J. Corkill, and M. Cohen

Crystal Structure of Stage 1 Iodine Intercalated Superconducting $IBi_2Sr_2CaCu_2O_x$

Physica C, Vol. 181, p.18 (1991).

The crystal structure of stage-1 iodine-intercalated superconducting $IBi_2Sr_2CaCu_2O_x$ has been determined by transmission electron microscopy to belong to the space group Pma2 with subcell lattice parameters $a = 5.4$Å, $b = 5.4$Å, and $c = 18.9$Å, and a structural modulation wavelength of 26Å. Intercalated iodine atoms alter the atomic stacking across Bi-O layers from the staggered configuration characteristic of superconducting $Bi_2Sr_2CaCu_2O_x$ to a vertically aligned configuration in $IIBi_2Sr_2CaCu_2O_x$. From the atomic spacings apparent in the images, it is concluded that the iodine layers bond to their neighboring Bi-O layers by van der Waals interactions.

31438 M RP

N. Kijima, R. Gronsky, X. Xiang, W. Vareka, A. Zettl, J. Corkill, and M. Cohen

Crystal Structure of Stage *n* Iodine Intercalated Compounds $IBi_{2n}Sr_{2n}Ca_nCu_{2n}O_x$

Physica C, Vol. 190, p.597 (1992).

The crystal structure of stage-3 iodine-intercalated superconducting $IBi_6Sr_6Ca_3Cu_6O_x$ has been determined by transmission electron microscopy to belong to the space group Pma2 with lattice parameters $a = 5.4$Å, $b = 5.4$Å, and $c = 49.4$Å. Iodine atoms intercalated between every three Bi-O bilayers expand the distance between the Bi-O layers by 3.6Å and alter the atomic stacking across Bi-O layers from the staggered configuration characteristic of host superconducting $Bi_2Sr_2CaCu_2O_x$ to an aligned configuration characteristic of stage-1 iodine-intercalated superconducting $IBi_2Sr_2CaCu_2O_x$. Higher stage intercalation has also been observed as stacking faults which predominantly contain both stage-2 and stage-3 phases. The space groups and *c*-axis dimensions of the higher stage phases have been deduced to be Pma2 with $c = 3.6 + 15.3n$ Å when stage number n is odd, and Bbmb with $c = 2(3.6 + 15.3n)$ Å when n is even.

31437 M R

N. Kijima, R. Gronsky, X. Xiang, W. Vareka, A. Zettl, J. Corkill, and M. Cohen

Crystal Structure of Stage 2 Iodine Intercalated Superconducting $IBi_4Sr_4Ca_2Cu_4O_x$

Physica C, Vol 184, p.127 (1991).

The crystal structure of stage 2 iodine intercalated superconducting $IBi_4Sr_4Ca_2Cu_2O_x$ has been determined by transmission electron microscopy to belong to the space group Bbmb with lattice parameters, $a = 5.4$ Å, $b = 5.4$ Å, $c = 68.5$ Å. Iodine intercalates between every other Bi-O bilayer of the superconducting crystal, expanding the distance between the contiguous Bi-O layers by 3.6 Å and altering the atomic stacking across these Bi-O layers from the staggered configuration characteristic of superconducting $Bi_2Sr_2CaCu_2O_x$ to the registered configuration characteristics of stage 1 iodine intercalated superconducting $IBi_2Sr_2CaCu_2O_x$.

---

unnumbered M No

X.-D. Xiang, W.A. Vareka, A. Zettl, J.L. Corkill, M.L. Cohen, N. Kijima, and R. Gronsky

Metallization of the Resistivity Tensor in $Bi_2Sr_2CaCu_2O_x$. Through Epitaxial Intercalation

Physical Review Letters, Vol. 68, #4, p.530 (1992).

We have used iodine intercalation to alter the interplane interaction and the anisotropic resistivity tensor of the oxide superconductor $Bi_2Sr_2CaCu_2O_x$. Real-space transmission electron microscopy images confirm that iodine is epitaxially intercalated between the Bi-O layers. In the normal state above T_c, the metallic CuO_2 plane sheet resistance is unaffected by intercalation, while the out of plane conduction is dramatically changed from semiconductorlike to metallic like. This result is inconsistent with some of the theoretical predictions based on holon-spinon scattering.

33500 M No

V. Radmilovic, M.A. O'Keefe, and G. Thomas

Imaging of SiC in Metal-Matrix Composites

Proc. 10th Eu. Cong. on Elec. Micros., Vol. 2, p.449 (1992).

Many polytypes of SiC have been reported in investigations by x-ray. However, transmission electron microscopy techniques, under conditions described by Smith and O'Keefe have certain advantages over the x-ray diffraction in determination of the lattice periodicity, especially in resolving fine structural details, e.g. stacking sequences, mono-layer twinning, polytypes, etc. The even more complex problem is imaging of SiC in "real-world" materials, as a metal matrix composite (MMC), where SiC is embedded in a metal matrix. This paper is, we believe, the first attempt in matching simulation to an actual experimental image of SiC in MMC. MMC used in this work was Al-8.5wt.%Fe - 1.3wt.%V-1.7wt.% Si alloy containing 15wt.% of SiC particulates, processed by powder metallurgy technique.

33428 M No

C.P. Burmester, L.T. Wille, and R. Gronsky

Monte Carlo Simulation of Oxygen Ordering in the High Temperature Superconductor $YBa_2Cu_3O_z$

Proc. 6th SIAM Conf. on Parallel Processing

The development of Monte Carlo single instruction multiple data (SIMD) parallel algorithms for the study of oxygen ordering in the basal plane of $YBa_2Cu_3O_z$ from first principles is described. In particular, implementation of the Ising model with short-range pair interactions on the SIMD architecture MasPar MP-1 (DEC mpp-12000) series of massively parallel computers is demonstrated. Special attention is given to methods which optimize processor array use and the particular pitfalls associated with parallel implementation of the Monte Carlo technique associated with the violation of ergodicity and coupling of the system Hamiltonian dynamics with the processor update period.

---

unnumbered M No
C.J.D. Hetherington and U. Dahmen

An Optical Moire´ Technique for the Analysis of Displacements in Lattice Images

Proc. 10th Pfefferkorn Conf., (anticipated publ. 1993)

High resolution electron microscopy is a means for imaging not only the local structure at a defect or interface but also the displacement field in the surrounding lattice. However, in general it is difficult or tedious to analyze this field which can extend across the entire micrograph. The optical moire´ technique, which is based on interference effects between the experimental lattice image and an artificial reference lattice allows a rapid and accurate measurement of the displacement. Small violations of translation, rotation or mirror symmetries give rise to large changes in the periodicity or orientation of the moire´ pattern. The different types of patterns: simple rotation, simple parallel and "mixed", are then best interpreted by reference to reciprocal space vectors of the component lattices. Displacements in the experimental image revealed by the moire´ pattern represent displacements in the actual specimen under certain conditions. This technique therefore provides a means for detecting lattice defects and for measuring lattice rotations and rigid body shifts.

30691 M RP
M.A. O'Keefe, and J. Spence

Resolution in Atomic Resolution Electron Microscopy

Proc. EMSA, p.498 (1991).

The Rayleigh resolution criterion was developed for incoherent imaging conditions and cannot, in general, be applied to coherent high-resolution TEM. In fact, the Rayleigh criterion may lead to paradoxical results since it consider only two scatterers and does not account for the signal to noise ratio. For the case of strong multiple scattering in HRTEM lattice imaging, the only general relations that can be assumed between the image of a specimen and its projected crystal potential are those imposed by symmetry, and the local HRTEM column approximation. The effects of limited resolution may produce an image of lower symmetry than that of the object.

30661 M No
R. Kilaas

Defect Modeling in HRTEM Image Simulation

Proc. EMSA, p.528 (1991).

One practical problem in HRTEM image simulation is the creation of atomistic models of defect structure. The ideal crystal structures are readily represented by a relatively small number of basis atoms and the crystallographic space group. On the other hand, the specks of grain boundary between two crystals requires the atomic location of possibly thousands of atoms, and a HRTEM simulation program will need all this information before a calculation can be carried out. Users comfortable with writing computer code will write a computer program to generate the hundreds or thousands of atomistic locations, while others may be forced to enter the data by hand or search around for a ready made program that can generate the required data. To the author's knowledge, no such suitable program is readily available. There are existing programs that will generate geometric interface models, but these programs were designed to create input to atomistic relaxation calculations, not as generalized tools for creating defect structures.

30693 M No
M.J. Witcomb, U. Dahmen, M.A. O'Keefe, and K.H. Westmacott

HREM Imaging of Single Unit Cell Carbide Precipitates in Pt-C Alloys

Proc. EMSA, p.572 (1992).

Dilute Pt-C alloys are prototypical for studying oversize carbide phase precipitation from interstitial solid solution. Earlier studies showed the essential function of quenched-in vacancies in the precipitation process. Vacancies play a dual, volume accommodation and structural role in the transformation by modifying both the habit plane spacing and stacking sequence. It was also shown how the precipitation sequence in interstitial Pt-C alloys is analogous to that in substitutional Al-Cu alloys. Initially a "GP zone" consisting of a monolayer plate of carbon atoms and vacancies forms. Atomic resolution images of the so-called α precipitates have confirmed their structure. During subsequent coarsening of the precipitates, α' platelets form. In the present contribution, simulated images based on this structure are compared with experimental images obtained at 800kV on the JEOL-1000 ARM. In addition to confirming the proposed precipitate structure, the results show the potential for successful imaging of precipitate structures containing light elements.

30692 A P

K. Downing, H. Meisheng, H. Wenk, and M.A. O'Keefe

Electron Crystallographic Determination of the 3-D Structure of Staurolite at Atomic Resolution

Proc. EMSA, p.540 (1991).

With current advances in electron microscope design, high resolution electron microscopy has become routine, and point resolutions of better than 2 Å have been obtained in images of many inorganic crystals. Although this resolution is sufficient to resolve interatomic spacings, interpretation generally requires comparison of experimental images with calculations. Since the images are 2-dimensional representations of projections of the full 3-D structure, information is invariably lost in the overlapping images of atoms from various heights. The technique of electron crystallography, in which information from several views of a crystal is combined, has been developed to obtain 3-D information on proteins. Application of the technique to HREM has producd "images" of sections through the crystal potential of the mineral staurolite. In these sections, all atoms are resolved, including oxygen.

30921 A No

M. Fendorf, S.E. Fendorf, D.L. Sparks, and R. Gronsky

Use of TEM Characterization of Reactions of MnO_2 with Cr(111) and Al(111)

Proc. EMSA, p.634 (1991).

Metal sorption is an important aspect of surface environmental processes which dramatically affect environmental quality. Sorption phenomena are active in transport and oxidation/reduction reactions, biotransformation, and in determining the ultimate fate of metals in surficial systems. Although oxide materials often only constitute a small fraction of the solid composition in surficial environments, their high surface area, reactivity, and coating abilities make them extremely influential in sorption. Surface precipitation provides a model for the sorption of hydrolyzable metal ions at the solution/solid interface, and was successfully used to explain observed trends in the reaction of various metal ions on oxide surfaces.

30690 A R
T.D. Nguyen

Hexagonal Phase in Tensile LPCVD Poly-Si Film

Proc. EMSA, p.812 (1991).

Polycrystalline silicon (poly-Si) films have found many applications in integrated circuits, actuators and sensors. Important considerations in the processing of these devices are structural stability and repeatable mechanical properties of the film. The texture and stress state of the films depend strongly on the microstructures and morphology of the films. Tensile films, which are preferred to compressive buckling, are characterized by equitaxial grain morphology, while compressive films are characterized by columnar grain growth during deposition.

32064 A No
K. Krishnan

Electronic Structure Changes Associated with Magnetic Transitions in Binary Alloys: An Exploratory PEELS Study

Proc. EMSA, Vol. 50, p.1260 (1992).

The Curie temperature of a disordered alloy may differ from that of a partially ordered system. Alternatively, magnetism can influence chemical order and produce substantial changes in the phase diagram. These results have been established by a detailed investigation of the $Co_{1-x}Pt_x$ system and the entire phase diagram, including magnetic and chemical effects, have been calculated and shown to be in good agreement with experimental data. In addition, ultrathin multilayers of Co/Pt show perpendicular anisotropy but the origin of this unique property is not well understood. Recently, we have shown that the *d*-electron density of states of a range of $Cu_{1-x}Pd_x$ alloys, based on measurements of $L_{3,2}$ transitions ("white lines" - WL) in electron energy-loss spectroscopy (EELS), is critically dependent on short-range order (SRO). In this paper we present results of the combined effect of magnetic and chemical order on the *d*-hole count, as measured by the normalized Co WL intensities, in four different Co/Pt alloys.

---

unnumbered A No
Z. Liliental and R. Kilaas

Phase Segregation in GaAs Layers Grown at Low Temperature

Proc. EMSA, p.860 (1991).

GaAs device and circuit performance may be impaired by substrate conduction. One such effect, called sidegating, leads to undesirable cross-talk between neighboring devices. This problem can be avoided by isolating the active device layer from the substrate with A GaAs buffer layer grown by molecular beam epitaxy (MBE) at low temperature (LT GaAs). The LT GaAs layers show high resistivity, a large trap density, and breakdown strengths about ten times that of semi-insulating GaAs. These layers are grown as a substrate temperature of ~200°C. A large (~1 at .%) excess of As in these As grown layers causes an increase (~0.1%) in the GaAs lattice parameter.

32086 M, I No
U. Dahmen, N. Thangaraj, and P. Lours

Applications of HREM to the Structural Analysis of Crystalline Interfaces

Proc. EMSA/MAS, 50, 114 (1992).

The investigation of the atomic structure of crystalline interfaces by HREM has recently become more prominent because of greatly improved resolution of modern electron microscopes, better means of sample preparation and wider availability of more generally applicable atomistic simulation procedures. As a result, a number of recent investigations have reported new and interesting features of crystalline interfaces and compared them with models based on atomistic, crystallographic or elastic theories. Examples of such features are stand-off dislocations in metal-ceramic and ceramic-ceramic interfaces, structural multiplicity of grain boundaries, solute segregation to selected facets, grain boundary microfaceting and dissociation and elastic distortion fields around interfacial ledges.

32087 I, M R

M.J. Witcomb, M.A. O'Keefe, C.J. Echer, C. Nelson, J.H. Turner, U. Dahmen, and K.H. Westmacott

An Atomic Resolution Study of a Carbide Phase in Platinum

Proc. EMSA/MAS, 50, 20 (1992).

Under normal circumstances, Pt dissolves only a very small amount of interstitial carbon in solid solution. Even so, appropriate quench/age treatment leads to the formation of stable-Pt_2C (100) plate precipitates. Excess (quenched-in) vacancies play a critical role in the process by accommodating the volume and structural changes that accompany the transformation. This alloy system exhibits other interesting properties. Due to a large vacancy/carbon atom binding energy, Pt can absorb excess carbon at high temperatures in a carburizing atmosphere. In regions of rich-in carbon and vacancies, another carbide phase, Pt_7C, which undergoes an order-disorder reaction was formed. The present study of Pt carburized at 1160°C and aged at 515°C shows that other carbides in the Pt_xC series can be produced.

---

un-numbered M No

J.B. Liu, J.Z. Duan, and R. Gronsky

Structural and Compositional Effects on the Electron Migration Properties of Al-Cu Alloy

Proc. EMSA/MAS, p.1420 (1992).

Aluminum and aluminum-based alloys are typically used as the metallization interconnections in LSI and VLSI silicon-based integrated circuits. Important factors affecting the lifetime and reliability of these interconnections in IC devices are the individual microstructures, device layer combinations, electron migration, and stress migration that occur during their fabrication and their in-service application. There are many possible remedies for each of these factors. The use of bias sputtering or "planarization" has been shown to improve the quality of the interconnection greatly. Recently, some studies have revealed a new planarization technique involving sputter deposition of Al alloys at elevated temperature without any substrate bias, combined with a TiN precoating to reduce the migration of Al atoms. In this paper, the microstructure of Al-0.2Cu/TiN/SiO_2/Si under optimum lifetime conditions is assessed, and a mechanism of void formation is proposed to explain the observations.

32088 M R

M.A. O'Keefe, and V. Radmilovic

Extension of the Thin Crystal Condition by Small Crystal Tilts: Why HREM Images of SiC Polytypes Always Look Tilted

Proc. EMSA/MAS, p.116 (1992).

Both experimental and simulated high-resolution electron microscope images of silicon carbide polytypes commonly exhibit symmetry changes in thicker crystal regions compared to the perfect (projected) space group symmetry of images from thin crystals. However, the changes predicted by simulation, and those found experimentally, are quite different. In simulated images the thin-crystal image degrades with increasing sample thickness because of the action of second-order interferences. However, in experimental images the degradation is because of crystal tilt. It appears that microscopists tend automatically to tilt SiC specimens in order to achiever "better looking" images by extending the thin-crystal condition.

32129 A P

K. Tsai, A. Schwartzman, R. Gallego, M. Ortiz, M.A. O'Keefe, and K.-S. Kim

Determination of the Strain Field From an HREM Image of a Si Lomer Dislocation

Proc. EMSA/MAS, p.144 (1992).

A novel approach to quantitative deformation characterization of high-resolution electron microscopy (HREM) defects images has been developed. The essential principle of this technique, called Computational Fourier Transform Deformation (CFTD) analysis, is to extract an accurate displacement field about a defect from its HREM image using Fourier transformation procedures. The methodology's unique feature is to digitize the defect image and compute the Moire´ pattern, from which the displacement field is obtained, without the need for an external reference lattice image, normally associated with the interference phenomena.

---

unnumbered A No
W.J. Moberly, D.B. Miracle, and S. Krishnamurthy

Deformation at Interfaces of Ti-6Al-4V/SiC Fiber Composites

Proc. EMSA/MAS, p.158 (1992).

Titanium-aluminum alloy metal matrix composites (MMC) and Ti-Al intermetallic matrix composites (IMC), reinforced with continuous SCS6 Sic fibers are leading candidates for high temperature aerospace applications such as the National Aerospace Plane (NASP). The nature of deformation at fiber/matrix interfaces is characterized in this ongoing research. One major concern is the mismatch in coefficient of thermal expansion (CTE) between the Ti-based matrix and the SiC fiber. This can lead to thermal stresses upon cooling down from the temperature incurred during hot isostatic pressing (HIP), which are sufficient to cause yielding in the matrix, and/or lead to fatigue from the thermal cycling that will be incurred during application. A second concern is the load transfer, from fiber to matrix, that is required if/when fiber fracture occurs. In both cases the stresses in the matrix are most severe at the interface.

30549 M P
R. Gronsky

Advancing Conventional High-Resolution Electron Microscopy

Proc. EMSA/MAS, p.652 (1991).

Due to the exceptional performance of most modern commercial transmission electron microscopes, the achievement of phase-contrast imaging resolution in the sub-2Å range is today a routine exercise, provided the samples are compliant. Nonetheless, there remains room for improvement, and the purpose of this manuscript is to highlight procedures that might be employed by the practicing microscopist for advancing conventional high resolution electron microscopy.

30618 M RP
K. Krishnan, and C. Echer

Measurements of Ionization Cross Sections for Electron Energy Loss Microanalysis Under Well Defined Scattering Conditions

Proc. EMSA/MAS, p.259 (1991).

Partial cross-sections required for electron energy-loss microanalysis have been measured for a series of high purity single crystal standards. For each sample four different scattering geometries were used. The experimental data were compared with theoretical calculations using both standard hydrogenic model and parametrized Hartree-Slater cross sections. Best agreement between theory and experiment were observed for experiments performed in diffraction mode (image coupling) with the probe convergence angle (0.84 mrad) much smaller than the spectrometer collection angle (6.84 mrad). In addition, specimen thickness from the region of microanalysis were measured by convergent beam electron diffraction. Absolute cross-section based on these measurements are also currently being determined.

---

unnumbered A No
W.J. Moberly, J. Busch, and D. Johnson

HVEM of Crystallization of Amorphous TiNi Shape Memory Films

Proc. EMSA/MAS, part 1, p.30 (1992).

TiNi alloys, well-known for their shape memory properties that arise due to a martensitic transformation, have recently been considered for application as thin film actuators. Although various methods of thin film preparation have been considered, deposition via d.c. magnetron ion sputtering provides for reproducible film formation as well as possible integration of a TiNi film as a micromachine with a semiconductor device.

32002 M No
K. Krishnan

Ceramic Microstructures and Their Elucidation by Imaging, Diffraction and Spectroscopic Methods

Proc. EUREM '92, Vol. 2, p.363 (1992).

The development and potential utilization of ceramic materials is dependent on a systematic effort involving processing, characterization and appropriate property measurements. The methods of characterization are numerous and it is important to employ the one that is appropriate to the problem both in terms of its information content and the achievable level of resolution. With the incorporation of fine probe forming capabilities in a transmission electron microscope and the development of related diffraction, imaging and spectroscopic methods, it is now possible to obtain structural and chemical information from the same region of the sample at high spatial resolution. In this review, recent advances along with representative examples in the application of high resolution electron microscopy (HREM), convergent beam electron diffraction (CBED), low atomic number element microanalysis by x-ray emission spectroscopy (XES), fine structures in electron energy-loss spectroscopy (EELS), and specific site occupany determination by channeling experiments are discussed.

30928 M R
M. Fendorf, M. Tidjani, C.P. Burmester, L.T. Wille, and R. Gronsky

Non-Stoichiometric Defects in YBaCuO Thin Films

Proc. Europ. MRS, p.771 (1992).

Defects in superconducting YBaCuO thin films deposited by laser ablation are investigated by high resolution transmission electron microscopy. Micrographs reveal numerous defects in the YBaCuO film, falling into four basic classes. One of these is an interesting, non-stoichiometric helical defect structure which possibly corresponds to a growth-related screw dislocation. In general, defects in the YBaCuO film are associated both with the growth geometry and local deviations in stoichiometry. Substrate surface geometry is seen to have a profound effect on the number and type of defects produced. Simulation of annealing transformations using a static lattice, three dimensional, Monte Carlo technique is carried out to gain further insight into specific defect formation mechanisms. The results of these studies suggest preparation conditions that are expected to lead to films with improved critical current densities.

31073 M No
C. Burmester, L. Wille, and R. Gronsky

Computer Modeling of Y-Ba-Cu-O Thin Film Deposition and Growth

Proc. Euro ICAM, p.313 (1991).

The deposition and growth of epitaxial thin films of $YBa_2Cu_3O_7$ are modeled by means of Monte Carlo simulations of the deposition and diffusion of Y, Ba, and Cu oxide particles. This complements existing experimental characterization techniques to allow the study of kinetic phenomena expected to play a dominant role in the inherently non-equilibrium thin film deposition process. Surface morphologies and defect structures obtained in the simulated films are found to closely resemble those observed experimentally. A systematic study of the effects of deposition rate and substrate temperature during in-situ film fabrication reveals that the kinetics of film growth can readily dominate the structural formation of the thin films.

33157 M P
M.A. O'Keefe

Using Coherent Illumination to Extend HRTEM Resolution: Why we Need a FEG-TEM for HREM

Proc. Microstructures of Materials Conf. (in press)

The resolution of a high-resolution transmission electron microscope (HRTEM) has traditionally been defined in terms of its Scherzer resolution limit at optimum defocus. However, even beyond the Scherzer limit, spatial frequencies can be transferred from the specimen to the image, out to the so-called information limit of the electron microscope. The information limit of the HRTEM is determined by the degree of energy spread in the electron beam used to illuminate the sample. Since a HRTEM equipped with a field-emission gun (FEG) will produce an electron beam of high coherence with little energy spread, it can achieve an improved information limit, and can thus be used to produce through-focus series of images containing information well beyond its nominal (Scherzer) resolution limit. Suitable computer processing of such series of images can produce composite images at resolutions approaching the microscope information limit. For such a FEG-TEM, combined with suitable computer image processing, resolution can approach 1Å.

33474 M No
U. Dahmen

Split Reflections from Broken Mirrors: Symmetry-Breaking in the Making of Materials Microstructures

Proc. Microstructures of Materials Conf., (in press, 1993).

The symmetry underlying the development of microstructure in materials is a global property with great practical uses in the design and analysis of precipitate distribution and morphologies, orientation relationships between crystals, properties of interfaces and textures and topographies of microstructures.

30729 M RP
N. Thangaraj, J. Reyes-Gasga, K.H. Westmacott, and U. Dahmen

Control of Texture During Vapor Deposition of Al on (111) Si

Proc. MRS, Vol. 221, p.81 (1991).

The growth of Al on (111) Si single crystal substrates by various techniques usually leads to films with (111) texture, sometimes with a small (100) component. Using x-ray diffraction and electron microscopy, the present study shows that the (100) texture component can be enhanced to the point of forming an oriented (100) continuous tricrystal structure. The formation of this texture is shown to be related to the presence of Cu. It is concluded that an understanding of heteroepitaxy must take into account the effect of chemistry in addition to the crystallographic criteria of lattice matching.

29284 M P
C. Burmester, M. Fendorf, L. Wille, and R. Gronsky

Theoretical Modeling and Experimental Characterization of Planar Defects in $Y_2Ba_4Cu_{6+x}O_{14+x}$

Proc. MRS, Vol. 209, p.807 (1991).

Crystallographic defects and phase transformations in the system $Y_2Ba_4Cu_{6+x}O_{14+x}$ are investigated by high resolution TEM and static lattice, 3 dimensional Monte Carlo computer simulations. High resolution images of partially transformed (x=2 to x=1) material reveal a prevalence of CuO planar defects (stacking faults) associated with the transformation and an absence of disturbance to the perovskite Ba-Y-Ba blocks. An atomic mechanism involving the intercalation and removal of extra CuO planes by partial dislocation climb, and requiring only a-b plane diffusion, is developed for the formation of such planar defects during changes in the layered YBaCuO crystal structure. Monte Carlo simulations based on the proposed transformation mechanism accurately reproduce the observed defects and known equilibrium structures.

29964 M P
T.D. Nguyen, D.A. Carl, D.W. Hess, M.A. Lieberman, and R. Gronsky

Structural and Interfacial Characteristics of Thin (<10 nm) SiO_2 Films Grown by Electron Cyclotron Resonance Plasma Oxidation on [100] Si Substrates

Proc. MRS, Vol. 223, p.75 (1991).

The feasibility of fabricating ultra-thin SiO_2 films on the order of a few nanometer thickness has been demonstrated. SiO_2 thin films of approximately 7 nm thickness have been produced by ion flux-controlled Electron Cyclotron Resonance plasma oxidation at low temperature on [100] Si substrates, in reproducible fashion. Electrical measurements of these films indicate that they have characteristics comparable to those of thermally grown oxides. The thickness of the films was determined by ellipsometry, and further confirmed by cross-sectional High-Resolution Transmission Electron Microscopy. Comparison between the ECR and the thermal oxide film shows that the ECR films are uniform and continuous over at least a few micros in lateral direction, similar to the thermal oxide films grown at comparable thickness. In addition, HRTEM images reveal a thin (1-1.5nm) crystalline interfacial layer between the ECR film and the [100] substrate. Thinner oxide films of ~5 nm thickness have also been attempted, but so far have resulted in non-uniform coverage. Reproducibility at this thickness is difficult to achieve.

30694 M, I P
U. Dahmen and K.H. Westmacott

TEM Characterization of Grain Boundaries in Mazed Bicrystal Films of Al

Proc. MRS, Vol. 229, p.167 (1991).

The structure and faceting behavior of near-90° <110> tilt grain boundaries in thin films of aluminum with a unique mazed bicrystal geometry is characterized by conventional, high-resolution and high-voltage electron microscopy. In this microstructure the absence of triple junctions allows grain boundaries to facet in optimum orientation (inclination) during annealing. The degree of anisotropy of the boundaries is expressed in the form of a rose plot. Small local deviations in misorientation are shown to be necessary to accommodate optimum boundary segments. The crystallographic symmetry inherent in this microstructure is apparent and utilized throughout the analysis.

31072 I, M R
P. Lours, K.H. Westmacott and U. Dahmen

Shape Transformation of Ge Precipitates in Al

Proc. MRS, Vol. 238, p.207 (1992).

Ge precipitates in Al-Ge alloys have been observed to undergo a transformation in shape during in-situ temperature cycling in a high voltage electron microscope. Octahedral precipitates with a parallel-cube orientation relationship spheroidized on heating and refaceted to the octahedral shape on cooling. This shape transformation was essentially conservative if the temperature excursions were kept small. These observations are discussed in terms of an interface roughening transformation.

---

unnumbered M No

P.K. Narwankar, M.R. Chandrachood, M. Fendorf, D.E. Morris, A.P.B. Sinha and R. Gronsky

Studies of Critical Current Density Enhancement in ($Ca_x Y_{1-x}$)$Ba_2Cu_4O_8$ (1:2:4)

Proc. MRS, Vol. 235, p.665 (1992).

Samples with the stoichiometry $(Ca_xY_{1-x})Ba_2Cu_4O_8$, x = 0, 0.1 were synthesized at $P(O_2)$ = 25 and 200 bar. High Resolution TEM images for the samples synthesized at 25 bar show a high density of planar defects as compared to almost defect free microstructure of $Ca_{0.1}Y_{0.9}Ba_2Cu_4O_8$ synthesized at 200 bar. The intragrain critical current density of the high defect density samples is, however, about 100 times lower than that of $Ca_{0.1}Y_{0.9}Ba_2Cu_4O_8$ synthesized at $P(O_2)$ = 200 bar.

---

unnumbered M No

A.F. Jankowski and M.A. Wall

The Stabilization of Face-Centered-Cubic Titanium

Proc. MRS, Vol. 238, p.297 (1992).

The artificial layering of metals can change both physical and structural characteristics from the bulk. The stabilization of such phases often occurs when the component layers are constructed on a nanometric scale. The sequential layering of nickel and titanium has produced the formation of a previously unreported face-centered cubic (fcc) phase of titanium.

31609 M R

Z. Weng, R. Gronsky, J. Lou, and W. Oldham

Silicon on Insulator Interface Structures in Selective Epitaxial Growth

Proc. MRS, Vol. 238, p.707 (1992).

Silicon on insulator structures were formed by the selective epitaxial growth (SEG) of silicon and the epitaxial lateral overgrowth (ELO) of oxide shapes using an LPCVD hot-walled reactor at 850° C. The homoepitaxial interface changed character with modifications of the gas composition during the in-situ pre-epitaxial bake at 900° C. HREM images show ellipsoid-shaped inclusions lying along the homoepitaxial interface for silicon growth conducted with no dichlorosilane (DCS) flow during the prebake in H_2. SIMS analysis indicates a large oxygen, fluorine, and carbon concentration at the interface. For structures grown with a small DCS flow in addition to H_2 during the prebake, the homoepitaxial structural defects and the oxygen, fluorine and carbon peaks are removed.

32513 M No

C. Burmester, L.T. Wille and R. Gronsky

Simulation of Vortex Line Pinning by Defects in the Y-Ba-Cu-O System

Proc. MRS, Vol. 275, p.819 (1992).

The finite temperature properties of a two-dimensional flux lattice are studied by Monte Carlo simulations, with particular attention to the effects of twin boundaries. The parameters selected are appropriate for the $YBa_2Cu_3O_7$ high temperature superconducting system. The intrinsic properties of the vortex state are investigated by monitoring system evolution at fixed temperature and applied magnetic field. By varying temperature, the loss of type-II superconductivity via fluxoid lattice melting is also examined. The introduction of model defects induces the creation of metastable and glassy states which reduce overall hexatic order but are found to enhance system resistance to flux-lattice melting.

31024 A , M No
C. Burmester, M. Fendorf, L. Wille, and R. Gronsky

High Resolution Electron Microscopy of Intercalated Phases in the Y-Ba-Cu-O System

Proc. MRS, Vol. 238, p.835 (1992).

High resolution transmission electron microscopy (HRTEM) is used to investigate the transformation mechanism responsible for the occurrence of the many stable layered phases in the psuedo-binary $Y_2Ba_4Cu_{6+x}O_{14+x}$ system. In particular, HRTEM results are compared with microstructural configurations generated by an earlier theoretical study which modeled this transformation by means of an intercalation mechanism.

32512 M No
C. Burmester, L. Wille, and R. Gronsky

Monte Carlo Simulations on SIMD Computer Architectures

Proc. MRS, Vol. 278, p. 3 (1992).

Algorithmic considerations regarding the implementation of various materials science applications of the Monte Carlo technique to single instruction multiple data (SIMD) computer architectures are presented. In particular, implementation of the Ising model with nearest, next nearest, and long-range screened Coulomb interactions on the SIMD architecture MasPar MP-1 (DEC mpp-12000) series of massively parallel computers is demonstrated.

33478 M P

F.M. Ross, R. Hull, D. Bahnck, J.C. Bean, L.J. Peticolas, R.R. Kola and C.A. King

Changes in Electronic Device Properties During the Formation of Dislocations

Proc. MRS, Vol. 280 (in press, 1993).

We describe the results of an investigation into the formation and properties of dislocations in electronic devices. We have made electron transparent specimens from metastable GeSi/Si p-n junction diodes and introduced dislocations into the devices by heating *in situ* in the electron microscope. A modification made on the specimen holder for our microscope enables us to measure the characteristics of these devices while they remain under observation in the microscope. We can therefore observe the changes in the electrical properties of the devices as dislocations form. We confirm that the introduction of dislocations has a deleterious effect on parameters such as the reverse leakage current through a diode. However, the magnitude of the effect we observe cannot be explained by a generation-recombination process and instead, we suggest a model based on the creation of point defects or the diffusion of metals during the formation of dislocations. We also consider the kinetics of dislocation formation, and in particular how the extent of dislocation formation in a device depends on the subsequent processing steps which it undergoes.

31270 M No

X. Xiang, W. Vareka, A. Zettl, J. Corkill, T. Barbee, M. Cohen, N. Kijima, and R. Gronsky

Tuning High T_c Superconductors via Multi-Stage Intercalation

Science, Vol. 254, p.1487 (1991).

Multistage intercalation has been used to tune the interaction between adjacent blocks of CuO_2 sheets in the high-T_c (high superconducting transition temperature) superconductor $Bi_2Sr_2CaCu_2O_x$. As revealed by atomic-resolution transmission electron microscopy images, foreign iodine atoms are intercalated into every *n*th BiO bilayer of the host crystal, resulting in structures of stoichiometry $IBi_{2n}Sr_{2n}Ca_nCu_{2n}O_x$ with stage index *n* up to 4. An expansion of 3.6 Å for each intercalated BiO bilayer decouples the CuO_2 sheets in adjacent blocks. A comparison of the superconducting transition temperatures of the pristine host material and intercalated compounds of different stages suggests that the coupling between each pair of adjacent blocks contributes ~5 K to T_c in $Bi_2Sr_2CaCu_2O_x$.

29216 M No

L. Wille, C. Burmester, P. Sterne, R. Gronsky, B. Ahn, V. Lee, R. Beyers, T. Gur, and R. Huggins

Oxygen Ordered Superstructures and Domain Formation in $YBa_2Cu_3O_{7-x}$

Proc. Topical Materials Conf., p.765 (1991).

In spite of a good deal of recent effort, the thermodynamic stability and kinetics of formation of ordered O-Cu-O chains in the basal plane of $YBa_2Cu_3O_{7-x}$ remain unclear. Because the chain disordering is associated with the orthorhombic-to-tetragonal phase transformation and the ensuing loss of superconductivity, a fundamental understanding of the nature of the oxygen-vacancy ordering has far-reaching implications for materials preparation and optimization.

---

un-numbered M No

R.S. Kedia, T.M. Lillo, Q. Horn, M.R. Plichta, and S.A. Hackney

Edge Instabilities in Thin Plates with Spatial Variations in Thickness

Scripta Met. et Mat.

The morphological stability of two dimensional structures has far-reaching consequences in a variety of materials problems. For example, the time dependent behavior of lamellar composite materials and thin coatings at elevated temperature can be directly related to the morphological integrity of the two dimensional structure. Time dependent behavior can be expected when the two dimensional morphology is not the equilibrium morphology and a thermodynamic driving force exists for the thin layer to undergo a morphological change to a structure with a smaller surface area to volume ratio. In many cases, the change in morphology occurs by a diffusional instability at the edges of two dimensional structures. The edge instabilities of two dimensional structures have been studied in relation to microcrystalline thin film stability, thin plate stability, intergranular film stability, and crack healing in brittle materials.

---

unnumbered M No
W. Cao, G. Thomas, M. Carey, and A.E. Berkowitz

Characterization of Epitaxial Sputtered $Ni_xCo_{1-x}O$ Thin Films on α-Al_2O_3 Using Transmission Electron Microscopy

Scripta Met. et Mat., Vol. 25, p.2633 (1991).

Epitaxial CoO-NiO multilayers have been produced which show interesting structural and magnetic properties. The single NEEL temperature observed for <111> oxide multilayers grown on on α-Al_2O_3 together with similar results found for FeF_2-CoF_2 multilayers, suggest that the magnetic properties of different ionic antiferromagnets can be mixed through alloying. This prompted the current study to produce Ni_xCo_{1-x} thin films in order to study their magnetic properties. The structure of these films is discussed in this report.

---

unnumbered M No
S.A. Hackney

Experimental Observations on Θ Phase Growth Morphology During Interdiffusion at the Al/Cu Interface

Scripta Met. et Mat., Vol. 26, p.1125 (1991).

Interfacial reactions between materials which are brought into contact but are not in global thermodynamic equilibrium occur in a variety of materials science applications, such as diffusion bonding, coating/substrate interactions, composite materials, thin film metallization of semiconductors, and in thin film layered structures in electronic devices. The experimental study of the initial stages of this process of phase formation at a nonequilibrium interface may allow some understanding of the principles which control the microstructural development (and thus the properties) of this interfacial region. From a scientific point of view, such a study provides an opportunity to study solid-solid phase boundary behavior under very high driving forces for growth.

---

unnumbered M No
A. Bouzaher, J.L. Verger-Gaugry and R. Bonnet

Dilation Field of a Regular Hexagonal Network of Misfit Dislocations: Application to (111)Si/(111)$CoSi_2$

Scripta Met. et Mat., Vol. 26, p.1107 (1992).

Diffusion phenomena under stress control the movements of misfit dislocations at high temperatures, e.g., (Phil Mag. A, 56, 31, 1987 and Acta Met. et Mat., 38, 881, 1990). For a better understanding of the diffusion paths of vacancies and atomic species on each side of the interface, it is necessary to determine all the elastic dilatation field Θ since these paths are orthonormal curves to equi-dilatation surfaces. In addition, elastic interactions between all linear interfacial defects must be taken into account for an accurate description of Θ. A brief review of works involving the elastic field of interfacial dislocations with anon-planar deformation field shows in fact that no solutions exist yet in the literature for Θ, even for the simplest case of a regular hexagonal network of misfit dislocations, which is in practice a common case observed in transmission electron microscopy.

30874 M R
C.P Luo, U. Dahmen, M.J. Witcomb, and K.H. Westmacott

Precipitation in Dilute Cu-Cr Alloys: The Effects of Phosphorus Impurities and Aging Procedure

Scripta Met. et Mat., Vol. 26, p.649 (1992).

Precipitation in dilute Cu-Cr alloys has been studied extensively, in part because this alloy can be used as a model system for the investigation of the crystallography and interfaces in FCC-BCC phase transformations. Hall et al. first report needle- or lath-shaped Cr-rich precipitates with a $[335]_f$ habit plane and a variable orientation relationship ranging from Nishiyama-Wassermann (N-W) to Kurdjumov-Sachs (K-S). The present study has been undertaken to investigate the effects of the P impurities and aging conditions on the crystallography of the Cr precipitates.

29593 M P

C.P. Burmester, L.T. Wille, and R. Gronsky

Monte Carlo Study of Domain Formation in $YBa_2(Cu_{1-x}Fe_x)_3O_z$

Solid State Communications, 77, 693 (1991).

Upon progressive doping with Fe the $YBa_2(Cu_{1-x}Fe_x)_3O_z$ compound transforms from an orthorhombic to a tetragonal structure without an accompanying loss of superconductivity. This behavior has been interpreted by assuming that the tetragonal structure consists of many conflicting orthorhombic microdomains pinned by the Fe-atoms. Extending an Ising model previously used to model the undoped compound, we show by Monte Carlo simulation that such microdomains do indeed occur. The oxygen content is allowed to vary in the simulations, while the Fe-Cu sublattice is handled in the canonical ensemble (fixed Fe-content). The Fe-atoms are mobile and found to cluster along the <11> direction in precise agreement with experimental observations.

---

unnumbered M No

H. Hashimoto, Y. Makita, Y. Yokota, T. Ikuta, M. Hashimoto, and C.J.D. Hetherington

Observations on Quick Fluctuation of Atom Images of Si Crystal Lattice Under 800 kV Electron Irradiation

Ultramicroscopy, 39, p.171 (1991).

The movement of atom images of a Si crystal under 800 kV electron beam irradiation has been recorded with the 1 MeV atomic resolution electron microscope at UC Berkeley equipped with a TV image viewing and video recording system. The small, rapid movements and contrast changes during 1/30 s have been revealed by taking the difference between two successive images which are recorded in each frame of the TV tape and processed. The difference between successive images has been displayed in real and prolonged time.

---

un-numbered M No
S.A. Hackney, T.M. Lillo, R.S. Kedia, Q.C. Horn and M.R. Plichta

Edge Instabilities in Thin Plates Studied by *In Situ* Transmission Electron Microscopy

Ultramicroscopy

The morphological instability of thin foil edges at elevated temperature is studied by *in situ* TEM. Quasi-periodic instabilities in the edge profile are observed to develop with a distinct growth direction perpendicular to the original foil edge direction. This results in the development of relatively tick rods perpendicular to the original edge. The rods are then observed to undergo spheroidization. The use of in situ techniques allows the direct study of the thickness changes associated with the formation and propagation of this instability. Such examination of the details of the thickness changes is critical to a full understanding and perhaps the control of the phenomenon.

32290 M P
B. Zhang, K.M. Krishnan, and R.F.C. Farrow

Crystallography of Co-Pt Multilayers and Nanostructures

Ultramicroscopy, (accepted 1992).

Atomically engineered nanostructures and multilayers of Co-Pt exhibit strong perpendicular anisotropy. This unique property, that determines their potential as a magneto-optic recording media, is dependent on a variety of microstructural parameters that include the overall crystallography, thickness of the layers, orientation, defect formation, interface reactions, etc. A series of Co-Pt multilayer samples with different thickness of the Co layer were studied by electron diffraction. It has been determined that the Co layers persist in the fcc structure up to a thickness of 50Å. As the thickness is varied from 3Å to 50Å in the multilayers, the Co film gradually relaxed to its bulk lattice parameter. (111) twinning and lattice strain at the interfaces between Pt and Co layers are also observed. The symmetry forbidden reflections observed at l/3 {224} positions in [111] zone diffraction patterns of the multilayer are due to (111) twinning and compositional modulations along the multilayer growth direction.

33720 M No
S. Paciornik, R. Kilaas and U. Dahmen

Assessment of Specimen Noise in HREM Images of Simple Structures

Ultramicroscopy (submitted, 1993).

Displacements of image spots representing atomic columns in a high resolution image may be due either to displacements of atomic columns or to specimen noise. The effect of specimen noise on the accuracy with which an atomic column can be located is assessed by evaluating the root mean square deviation of the intensity center of mass of image dots. Optimized methods for experimental assessment of this effect are developed and applied to simulated and experimental images.

29350 M P
M.A. O'Keefe, and R. Kilaas

Comments on "HRTEM-Bildkonstrastsimulation von Strukturen mit Punktdefeken in Speziellen Lagen"

Zeitschrift fur Kristallographie, 194, p.125 (1991).

We wish to point out that papers by Rahman (1988) and Rahman & Weichert (1990) contain a basic error in concept. In these papers, the authors seek to shorten the amount of computation necessary for a simulation of a high-resolution transmission electron microscope (HRTEM) image of a structure containing a defect, using as an example an oxygen vacancy in mullite. Unfortunately, the method used leads to errors in the exit-surface wave function, and hence, in the simulated image.

32399 M P
M.A. O'Keefe

"Resolution" in High Resolution Electron Microscopy

Ultramicroscopy, Vol. 47, p.282 (1992).

In the field of high resolution transmission electron microscopy (HRTEM), the term "resolution" has come to hold a number of different meanings. The present work reviews the various definitions of HRTEM resolution, derives theoretical expressions for resolution, and suggests how high resolutions may be attained in practice.

29590 M No
J.G. Ulan, R. Gronsky, and R. Szostak

Sensitivity of Iron Silicate Morphology and Crystallinity to Synthesis Gel Composition

Zeolites, Vol. 11, 466 (1991).

Electron microscopy has been applied to the study of iron silicates with the ZSM-5 structure. The microstructure and crystallinity of the products was very sensitive to alkali cation concentration and the SiO_2/Fe_2O_3 ratio of the initial crystallization gel. In all cases these materials crystallized as aggregates consisting of a shell of fused crystallites encasing smaller particles. The addition of alkali cations resulted in the crystallization of larger aggregates. Although the smaller particles within the aggregates were primarily crystalline, amorphous regions indicative of occluded gel were found inside aggregates which appear highly crystalline when examined by x-ray diffraction.

29591 M No
J.G. Ulan, R. Gronsky, and R. Szostak

Compositional Heterogeneity in Iron Silicate Molecular Sieve Syn-Gas Catalysts

Zeolites, Vol. 11, p.472 (1991).

Analytical electron microscopy has been utilized to examine iron silicates with the ZSM structure. The sensitivity of the iron distribution to synthesis gel composition was studied. The addition of a small excess of alkali cations to the initial crystallization gel resulted in large deviations in product iron distribution. Such an iron distribution would produce heterogeneous iron particle size distributions and must be considered in choosing these materials for catalytic processes.

---

un-numbered A No
H.R. Smith, B.J. Bramlett, C. Echer, and B.A. Dixon

Analysis of Selenium Granules in Aeromonas Hydrophilia

Proc. EMSA, p.324 (1991).

Selenium (Se) is a naturally occurring nonmetallic element found in the environment as a result of fossil fuel combustion and industrial and agricultural processes. Although it is an essential trace element for plants and animals, high levels of soluble Se in agricultural drainage water have had deleterious effects on fish and waterfowl. The toxic forms of Se exist as selenate (+VI) and selenite (+IV) and both valence forms can be chemically reduced to insoluble, non-toxic elemental Se (0). A number of microorganisms are capable of reducing soluble Se to the zero valence state. Models have been proposed for using indigenous bacteria in water treatment systems to remove the toxic forms of Se via the reduction process. In order to realistically utilize this procedure, it is necessary to demonstrate that the soluble Se is converted to elemental Se.

---

un-numbered A No
J.L. Burns, C.J. Echer, and R.J. Spontak

Formation of Nanoclusters on Polymer Thin Films

Proc. 49th EMSA, p.1122 (1991).

Several different techniques are currently employed for producing thin polymeric films for study in transmission electron microscopy (TEM), but the two most common routes are (cryo) ultramicrotomy and thin-film casting. Sections obtained from embedded samples or at low temperatures are valuable in correlating observed microstructure with bulk physical properties, without concern over non-equilibrium issues. However, thin-film casting is often equally useful, especially if there exists an interest in structure morphology at surfaces, which may help to elucidate surface (e.g. adhesive) properties of the material. In either case, resulting thin films can be further processed on TEM grids prior to imaging. Normally this additional step requires subjecting a film to an elevated temperature (T) for a predetermined period of time (t). Unlike most metals which are annealed at relatively high temperatures (>500° C) and most biological systems which are heated to temperatures typically less than 100° and 400° C. Depending on molecular characteristics and physical properties, these films may become rubbery or fluid-like and their surfaces more active at these temperatures. A phenomenon that we have encountered under these conditions is the formation and aggregation of electron-dense clusters measuring tens of nanometers (nanoclusters). The objectives of this work are to characterize these nanoclusters and identify the kinetic mechanism by which they form.

---

un-numbered M No
A.N. Goldstein, C.J. Echer, and A.P. Alvisatos

Melting in Semiconductor Nanocrystals

Science, Vol. 256, p.1425 (June, 1992).

New physics occurs in semiconductors when one or more dimensions of the crystal are reduced to a size comparable to bulk electron delocalization lengths (tens to hundreds of angstroms). The properties of "quantum dots" or semiconductor nanocrystals are now being studied, as techniques to fabricate the crystallites are developed. Temperature-dependent electron diffraction studies on nanocrystals of CdS show a large depression in the melting temperature with decreasing size, as a larger fraction of the total number of atoms is on the surface. Thermal stability may play a role in determining the uses of semiconductor nanocrystals.

Please send a reprint of the paper(s):

Number	Author(s)	Title

Name_____ Date_____

Affiliation_____

Address_____

_____

Please send a reprint of the paper(s):

Number	Author(s)	Title

Name_____ Date_____

Affiliation_____

Address_____

_____

National Center for Electron Microscopy
U.C. Lawrence Berkeley Laboratory
1 Cyclotron Rd. Building 72
Berkeley CA 94720

National Center for Electron Microscopy
U.C. Lawrence Berkeley Laboratory
1 Cyclotron Rd. Building 72
Berkeley CA 94720

DISCLAIMER

National Center for Electron Microscopy
Lawrence Berkeley Laboratory
University of California
Berkeley, Ca 94720